IEEE Access
The journal for rapid open access publishing

Received September 14, 2015, accepted September 27, 2015, date of publication October 19, 2015, date of current version October 28, 2015.

Digital Object Identifier 10.1109/ACCESS.2015.2489865

Resource Management and Inter-Cell-Interference Coordination in LTE Uplink System Using Random Neural Network and Optimization

AHSAN ADEEL, HADI LARIJANI, AND ALI AHMADINIA
School of Engineering and Built Environment, Glasgow Caledonian University, Lanarkshire G4 0BA, U.K.
Corresponding author: H. Larijani (h.larijani@gcu.ac.uk)

ABSTRACT In orthogonal frequency division multiple access systems, inter-cell interference (ICI) can be considered as a collision between resource blocks (RBs), which can be reduced by employing a power control strategy at colliding RBs. This paper presents a random neural network (RNN) and a genetic algorithm-based hybrid cognitive engine (CE) architecture to reduce the ICI and achieve the coverage and capacity optimization in a long-term evolution uplink system. The embedded CE within eNodeB learns from the local environment about the effect of ICI on the reliability of communications. Consequently, the CE dynamically selects the optimal transmission power for serving users based on an experienced signal-to-interference-plus-noise ratio and an ICI on a scheduled RB in the subsequent transmission time intervals. The CE also suggests acceptable transmit power to users operating on the same scheduled RB in adjacent cells through the X2 interface (a communication interface between eNodeBs). The RNN features help the CE to acquire long-term learning, fast decision making, and less computational complexity, which are essential for the development and practical deployment of any real-time cognitive communication system. In six different test cases, the simulation results have shown improvements up to 87% in long-term learning and a quick convergence of the RNN as compared with artificial neural network models. Moreover, the gains of 7% in average cell capacity and 118% in system coverage have been achieved as compared with a fractional power control method.

INDEX TERMS Artificial neural network, coverage and capacity optimization, fractional power control, genetic algorithm, inter-cell interference, power control, random neural network.

I. INTRODUCTION

Cognitive radio (CR) systems with their inherent abilities of adaptation and reconfiguration are commonly described as intelligent wireless communication devices. The cognition capability enables radios to sense its operational electromagnetic environment, learn system behaviour, and plan intelligently. Future wireless systems with cognitive features will be able to reconfigure their radio parameters depending on the user requirements, surrounding environment, and equipment operational ability in order to move towards an optimized operational state [1].

In literature, inter-cell interference coordination (ICIC) and radio resource management (RRM) schemes have been extensively studied and researchers have proposed several solutions based on approaches from statistical, analytical, and classical network optimization schemes to self-organized approaches [2]–[4]. If the radio obtains knowledge of operational electromagnetic environment, user requirements, and parameters effecting the reliability of communication, then providing services such as autonomous computing and optimization could be achievable. Therefore, the cognitive or self-organizing network frameworks could provide an appealing solution for ICIC and RRM problems requiring minimum supervision.

In [5], the authors proposed an interference management scheme using cognitive base stations (CBSs) for LTE and discussed the insufficiency of traditional interference management schemes for isolated cell or a multi-cell LTE networks. The authors argued that CBSs could exploit their knowledge of radio-scene to intelligently allocate resources and to mitigate prohibitive co-channel interference. To make such designs possible, radio community has recommended

numerous solutions within the CR design space with different *a priory* knowledge assumptions and combination of various artificial intelligence (AI)/machine learning (ML) techniques [6]. The key required feature for such intelligent system is to have an effective learning capability, i.e. the ability to learn well and behave intelligently, which is critical to the performance of autonomously deployed CRs.

Training or exploration is the task by which a CE gets through the process of learning a desired systems' behaviour and capabilities. The training speed, accurate learning, available training samples, and computational complexity during this task are of paramount importance to the systems' operational performance and also limiting factors for CR to achieve optimal configuration settings in real-time. Researchers have made great effort to solve the CE training problems and demonstrated that a CE can be trained with in a reasonable amount of time and effort [7].

In the process of CE exploitation (testing), if the radio does not know any satisfactory solution to the current problem, then it will have no other option but to explore (train) again, which consumes time and energy. To avoid the process of retraining during radios operation, it is necessary to put the CE through all expected operating conditions in the training phase. However, it is practically impossible to explore all possible conditions as *a priori*. Therefore, a CE may face an unknown condition sooner or later and may require retraining. If the radio is operating in a critical mission, then it may not have time to retrain again and again [7]. Therefore, the capability of long-term learning is of great importance which enable CEs to adapt themselves with respect to severe changes in environment without the need of retraining.

Insufficiency of long-term learning along with the concurrent achievement of fast decision making and less complexity are the major limiting factors of existing AI/ML based cognitive approaches in literature. Recently, two hybrid CE architectures based on particle swarm optimization (PSO)+case-based system (CBS) and GA+CBS were presented in [8] and [9]. In these papers, the optimal radio parameters were determined considering the users' quality-of-service (QoS) preferences and dynamic electromagnetic environment. The CEs used PSO/GA based reasoning to explore optimal radio parameters in unknown cases and used CBS for known cases. These schemes have shown improvement in system response time but the priori characterizations of performance metrics were derived from analytical modelling. Therefore, limited learning, limited modelling assumptions, lack of ability to deal with non-ideal communication behaviours, and poor scalability are some of the limiting factors.

Researchers have proposed both supervised and unsupervised learning algorithms for ICIC and RRM. However, to the best of our knowledge, limited work has been conducted to concurrently achieve aforementioned CE design features. In contrast with existing AI/ML based approaches e.g. [10]–[12], RNNs inherent properties such as: (a) efficient computation (b) low complexity (c) energy-efficient hardware implementation (d) less dependency on network structure (e) strong generalization capability even with small training dataset, makes RNN a better choice for CE design [13].

RNNs have been used in many applications such as texture generation, video/image compression, image segmentation, target system recognition, vehicle classification, landmine discrimination etc. For a comprehensive survey of RNN and its applications, see [13]. The use of RNN for QoS driven routing protocol (i.e. cognitive packet network (CPN)) was presented in [14]. The authors in [15] extended their work on CPN and presented an innovative use of GA for dynamic adaptive routing in packet networks. Smart and adaptive approaches to CR and channel sharing have also been considered in [16] and [17].

In our previous work [18], [19], we addressed some of the CE exploration and exploitation challenges and presented the out-performance of RNN over ANN and hierarchical RNN over traditional RNN in terms of generalization, learning efficiency, and computational complexity. The work in [20] and [21] further addressed the convergence speed and local minima problems of gradient descent (GD) based RNN by implementing adaptive inertia weight particle swarm optimization (AIW-PSO), differential evolution (DE), and GA training algorithms. This paper has extended our previous research by presenting RNNs first application to the problem of LTE uplink RRM and ICIC. We review the existing state-of-the-art, research challenges involved, and present a novel RNN based power controller and interference management framework.

II. RELATED WORK AND CONTRIBUTIONS

In this section, we summarize the significance of power control in LTE uplink, shortcomings of 3rd generation partnership project (3GPP) defined FPC method, and discuss the analytical/AI/ML based RRM/ICIC schemes in literature to better highlight our contribution.

A. POWER CONTROL

In LTE uplink system, transmit power is one of the key and most influential parameters, which can address the challenges posed by channel fading, ICI, adjacent-channel interference (ACI), and user equipment (UE) excessive transmission power. Therefore, optimal power allocation has been one of the most researched topics and researchers concentration in LTE optimization. 3GPP defined uplink power control (PC) for LTE as a combination of open and closed loop components. The open loop power control (OLPC) is often known as FPC which sets the UE transmission power in a distributed manner. The FPC compensates slow changes of path-loss (PL) (including shadowing) and aims at reducing the PL perceived by the cell-edge users. The UE estimates the PL by measuring the downlink pilot signals and correspondingly changes the transmit power with respect to PL compensation factor (γ) defined by the eNodeB.

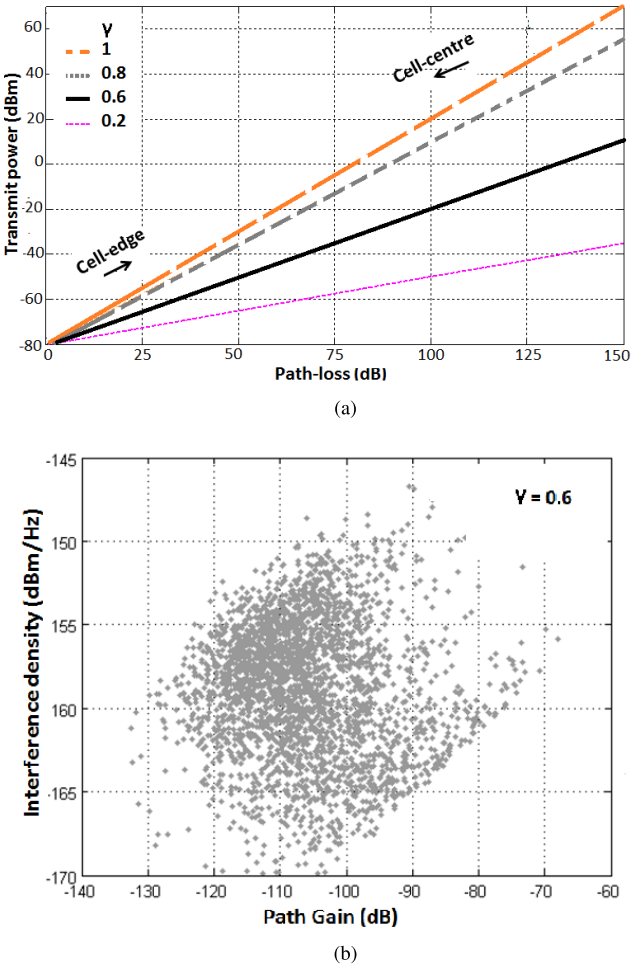

FIGURE 1. FPC based power allocation. (a) Path-loss vs. transmit power. Reduction in the path-loss compensation factor (γ) results in decreasing the transmit power of users with higher path-loss and vice versa. (b) Path-gain vs. interference density.

3GPP defined γ over the range of [0, 0.4, 0.5, 0.6, 0.7, 0.8, 0.9, and 1]. For a given FPC curve, moving from left to right, a trade-off between cell coverage and capacity exists. In two extreme cases, when $\gamma = 0$ (no PL compensation), all mobile stations (MSs') transmits at fixed power level and base station (BS) receives a wide range of power levels. This case leads to poor cell-edge users throughput due to users low transmission power. However, with full compensation power control (FCPC), $\gamma = 1$, BS receives signals with almost the same power level. Hence, this case improves cell-edge users throughput at the cost of reduced system capacity. This is due to high cell-edge users transmission power and corresponding increased interference with neighbouring cells. Therefore, it is difficult to ensure fairness between cell-centre and cell-edge users and indeed impossible to improve both capacity and coverage simultaneously. The proportional relationship between γ and the transmit power of users with higher PL is shown in Fig. 1 (a).

FPC method relies on the assumption that interference generated towards other cells is mostly because of cell-edge users. Fig. 1(b) clearly negates this assumption, where the interference samples are spread over the range of 20 dB for the same path-gain. It shows that users experienced the lowest path gain generated most of the interference is not true. This suggests to adjusting the power in order to compensate the generated interference rather than the path-gain [22].

B. RELATED WORK

The performance of uplink power control has been investigated intensively and researchers have shown different ways of optimizing power control parameters. Details about some of the competent methods are comprehensively presented in the following paragraphs.

The authors in [22] proposed an interference based power control scheme which dynamically adjust the target SINR in order to achieve a fixed level of interference at every cell. The evaluation of their proposed approach revealed average cell throughput gain of 16% while keeping the same cell-edge performance and an impressive gain of 57% in cell-edge throughput while keeping the same average cell throughput. The approach fails to simultaneously improve both capacity and coverage. In addition, it is also unclear that how the interference target could be dynamically set based on traffic statistics. The authors in [23] proposed a power level optimization method which maximizes the utility function using gradient descent technique. Their defined utility function estimates the throughput for each flow given the power level possible for transmission on each sub-carrier. However, the approach is based on computationally complex analytical modelling and exhibits no learning.

The authors in [24] investigated the potential of ICIC in terms of throughput, delay, and mobile station energy consumption gains that are theoretically possible by using multi-cell power control and multi-cell scheduling in wireless cellular systems. The authors investigated six different RRM/ICIC schemes namely Random, BSunc, radio network controller (RNC), RNC+BS, start index, and start index geometry weight. The authors compared the 50%-tile user throughput among the first four RRM algorithms and the cell-edge users throughput without a ICIC scheme, with start-index, and with start-index geometry weight schemes. The inefficient use of spectrum (i.e., frequency reuse factor N=3), extensive coordination between eNodeBs, and the requirement for backhaul communication and location information are some of the drawbacks in this approach. The detailed comparison with this approach is presented in Section V.D.4.

Brehm and prakash in [10] extended the work of [23] in a distributed self-organizing (SO) manner. The authors used support vector regression as a traffic predictor which assisted eNodeB in reallocating resources upon high traffic load. However, support vector machine (SVM) based approaches have some important practical questions such as the selection of kernel function and its parameters [25], training of multi-class SVM, high algorithmic complexity, extensive memory requirement, and slow speed during run-time. Recently, the authors in [26] presented a measurement driven ML paradigm for power control to manage interference in LTE-uplink.

Their work formulated the problem of optimally configuring the PL compensation factor of FPC scheme based on suitable periodic network parameters in a SO manner. A significant performance improvement up to 4 times has been shown but without any in-depth testing of proposed learning scheme under CE design requirements.

The authors in [11] proposed a reinforcement learning (RL) based decentralized solution for joint power control and cells association in heterogeneous networks. For realistic applications, the size of state-space could be so large that learning may take a long time and even become impossible in a reasonable time frame. As a result, the generalization over the state-space is necessary, which is insufficient in RL. A game theory based combined power and interference control framework for LTE-downlink is presented in [27]. However, this approach requires user-specific utility parameters, which can not always be acquired in many situations [2]. The authors in [12] proposed a Q-learning based aggregate interference control scheme and presented a framework which combined RL and ANN. However, ANN suffers from limited generalization, slow calculation rate at run-time, local minima, and over-fitting problems. Support vector regression for proactive resource allocation and stochastic-learning based gradient algorithm for adaptive power control is presented in [10] and [26] respectively. However, no testing under CE design requirements is shown. The authors in [28] proposed a self-organizing network (SON) framework in which eNodeB is modelled using fuzzy-RL to dynamically adjust the FPC parameters. However, it suffers from the same aforementioned RL limitations.

C. MOTIVATION

The RRM and ICIC solutions based on analytical modelling are mostly based on theoretical principles such as [23]. The implementation of such models requires large amounts of calculations which are to be calculated at very fine-grained time intervals. In addition, the analytical approaches suffer from limited learning capability, limited modelling assumptions, and poor scalability. In contrast, AI/ML based solutions are better suited for ICIC and RRM with minimum supervision requirements. The combined learning and reasoning processes are capable of dealing with non-ideal communication behaviours in a more competent way compared to analytical modelling. However, most of the presented AI/ML based cognitive or SO solutions in literature have not been investigated under CE design requirements. Also, when studying the interaction of ICIC with RRM mechanisms, very often the novelty is the modification of one RRM functionality in terms of channel allocation/frequency reuse pattern such as [24]. In these approaches part of the RBs are used with frequency reuse factor N=1 in the cell centre region and frequency reuse factor N=3 is applied in cell-edges. Therefore, such methods fail to comply with LTEs full frequency spectrum usage requirement. Moreover, their extensive information exchange, backhaul communication and location requirements adds more to the deployment cost and complexity.

D. CONTRIBUTIONS

The main contributions presented in this paper are:

1) Developed a novel, simple, and distributed RRM and ICIC framework. The framework reduces ICI with zero bandwidth loss, makes use of only one way communication (i.e., from Cognitive-eNodeB to adjacent eNodeBs), requires no backhaul communication, and uses only by default the available environmental measurement/configuration parameters at cognitive eNodeB for optimal RRM. The traditional FPC method has been replaced with a closed loop power control (CLPC) by embedding a CE in the eNodeB. This replacement aims to schedule optimal transmit power to the attached user equipments' (UEs) as well as suggest acceptable transmit power to the UEs served by neighbouring cells. The user specific power adjustment has a centralized control at the cognitive BS. MS feeds back the channel quality information (CQI) to the BS, which calculates optimal uplink transmit power level and instructs the MS to transmit at that level. The basic idea is to control the power to compensate for the generated interference to the system rather than the path-gain. The path-gain based power allocation is the assumption made by 3GPP for FPC based power allocation, which makes the joint CCO difficult.
2) Investigated the proposed CE architecture under essential CE design requirements such as long-term learning, fast decision making, and less computational complexity. The feasibility and reliability of proposed system in real-time cases has been checked, with training time constraints or where retraining may not be appropriate.
3) To minimize the cost function we have used GD and levenberg marquardt (LM) for training. In literature, researchers have mostly considered only GD as a training algorithm for RNN and ANN comparisons.
4) Detailed performance analysis was conducted a and comparison of proposed approach with ANN, FPC, and existing RRM/ICIC in terms of essential CE design requirements, capacity-coverage optimization, framework complexity, and deployment cost is presented.

III. RANDOM NEURAL NETWORK

RNN, a machine learning technique, made up of highly interconnected processing elements called as neurons, processes the information by their state response and learn from examples. The main objective of the RNN model is to transform the inputs into meaningful outputs, learn the input-output relationship, and offer viable solutions to unseen problems (a generalization capability). RNNs were first developed by Gelenbe in [29] as a new modified class of ANNs, representing the transmission of signals in a very similar form to biological neural networks, but offers more benefits and cope the limitations of ANNs. In RNN, a neuron can be seen as a queue with an exponential server having (service) rate μ and exciting/inhibition signals

as positive/negative customers. In case of no inhibition signal, RNN behaves as a classic M/M/1 queue.

A. MATHEMATICAL MODELLING

In RNN, the neuron exchanges the signal in the form of spikes. The potential (k) of each neuron represents its state that increases/decreases with respect to an incoming signal. A neuron u can receive exogenous signals positive/negative, modelled as Poisson arrival streams of rates Λ_u, λ_u, respectively. If a neuron receives an excitatory signal ($+1$), its potential increases and correspondingly decreases upon receiving inhibitory signal (-1). When the potential of neuron is equal to zero ($k_i = 0$), it is in idle state and when ($k_i > 0$), the neuron is excited. In the state of excitation, the neuron fires an excitatory spike that goes from neuron u to v of the network or to the outside world. In that case, the potential of neuron u decreases by one, whereas potential of neuon v increases by one. When neuron fires inhibitory spike, the potential of both neuron decreases by one. This firing is according to the Poisson process represented by the synaptic weights $w_{ij}^{+} = rP_{ij}^{+}$ and $w_{ij}^{-} = rP_{ij}^{-}$, where P_{ij}^{+} and P_{ij}^{-} are the probabilities of excitatory and inhibitory signals and r is the spikes firing rate. The w_{ij}^{+} and w_{ij}^{-} can be seen as the positive and negative rates of signal transmissions and these are the typical interconnections weights of a neural network that RNN learns through the process of learning or training. The average rate of +ive signals at neuron i ($\boldsymbol{\lambda_i^{+}}$), average rate of -ive signals at neuron i ($\boldsymbol{\lambda_i^{-}}$), and the probability that neuron i is excited ($\boldsymbol{q_i}$), are calculated using the following equations:

$$\boldsymbol{\lambda_i^{+}} = \boldsymbol{\Lambda_i} + \sum_{j=1}^{n} \boldsymbol{q_j w_{ij}^{+}} \tag{1}$$

$$\boldsymbol{\lambda_i^{-}} = \boldsymbol{\lambda_i} + \sum_{j=1}^{n} \boldsymbol{q_j w_{ij}^{-}} \tag{2}$$

$$\boldsymbol{q_i} = \frac{\boldsymbol{\lambda_i^{+}}}{\boldsymbol{r_i} + \boldsymbol{\lambda_i^{-}}} \tag{3}$$

1) NETWORK BEHAVIOUR IN STEADY STATE

if $0 \leq \boldsymbol{q_i} \leq 1$ for $i=1,2,3...,n$ then the stationary joint probability of network $\boldsymbol{p(k,t) = p_r = [k(t) = k]}$ can be written as:

$$\boldsymbol{p(k) = \Pi_{i=1}^{n}(1 - q_i)q_i^{k}} \tag{4}$$

2) NETWORK STABILITY

In [30], Gelenbe presented the mathematical usability and stability of RNN model. The author showed that network is stable if the potential of the signal increases with bounds, which can be guaranteed if a unique solution to non-linear equations (1-3) exists. However, existence of the solution implies its uniqueness and in feed-forward RNN, the solution always exists. A general RNN model in depicted in Fig. 2. Further in-depth details are comprehensively presented in [30].

B. RNN TRAINING ALGORITHMS

The capacity to learn from examples is one of the most desirable features of neural network models. The goal of training is to learn desired system behaviour and adjust the network parameters (interconnections weights) to map (learn) the input-output relationship and minimize the mean squared error (MSE). In [31], Gelenbe presented a learning algorithm for the recurrent random network model using gradient descent of a quadratic error function. The learning algorithm introduced in [31] for recurrent RNN can also be applied to feed-forward RNN, which has been used in this paper. In [20] and [21], we also implemented AIW-PSO, DE and GA based learning algorithms. However, in general, there is a trade-off among learning accuracy, convergence time, calculation time, and computational complexity. Further details and procedures are presented in [20], [21], and [31].

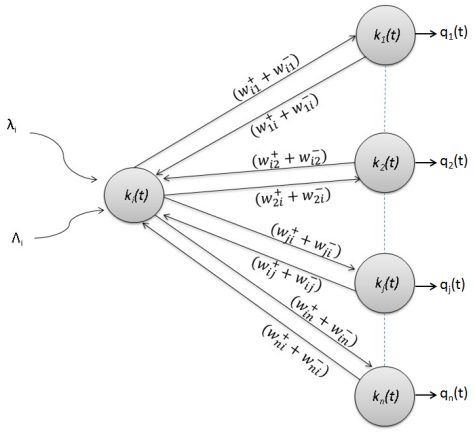

FIGURE 2. A feed-forward random neural network architecture.

IV. SYSTEM ARCHITECTURE

A. SYSTEM MODEL

In OFDMA system, ICI can be considered as a collision between RBs [24]. Fig. 3 illustrates such a collision model and the corresponding ICIC mechanism which aims to reduce the ICI at colliding RBs by employing a power control strategy. The modelled system has adopted 7-cell hexagonal layout (2 coexistent-10MHz Evolved Universal Terrestrial Radio Access frequency division duplexing systems) with omnidirectional antennas at the centre of each cell, depicted in Fig. 4. The RNN-CE is embedded inside the reference cognitive-eNodeB (C-eNodeB) which is responsible for monitoring and configuring the UE once it is attached and also the management of radio resources. In addition, the CE make decisions on acceptable transmit power of UEs served by adjacent eNodeBs. UEs are responsible for the enforcement of decisions made by C-eNodeB and sending environmental measurements back to C-eNodeB. Powers ($\boldsymbol{P}_0$, P1, P2, P3, P4, P5, and P6) are the configuration parameters or knobs of reference and adjacent eNodeB UEs, which are discussed in detail in Subsection-C and D.

B. MODELLING ASSUMPTIONS AND CALCULATIONS

The simulation is based on the assumptions and parameters of Evolved Universal Terrestrial Radio Access (E-UTRA)

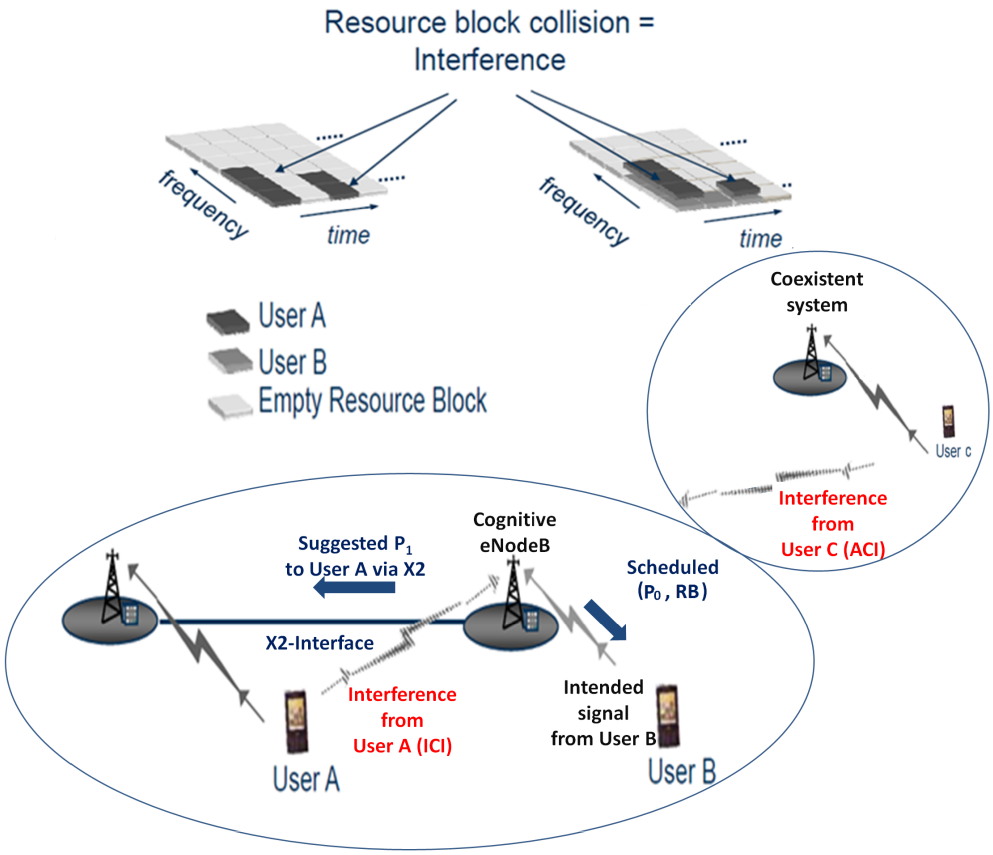

FIGURE 3. ICI caused by collision between resource blocks which are used simultaneously by several users in different cells and corresponding scheduling based on the experienced channel quality information and interference in subsequent transmission time interval.

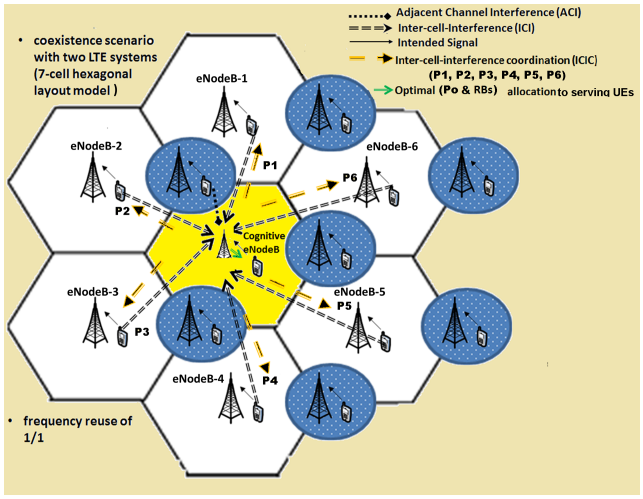

FIGURE 4. Proposed system model.

10MHz macro cell system used in the Qualcomm simulator. The systems are 100% loaded with frequency reuse of 1/1. The UEs are deployed randomly according to a uniform geographical distribution in the whole network region. The FPC settings, OFDMA LTE link-to-system level mapping, adjacent channel leakage ratio/unwanted spectrum mask are the same as given in Qualcomm STG(08)13 and 3GPP technical specification [32]. Further details about the system level simulation parameters are provided in Table 1.

At the beginning of simulation (for every snapshot), UEs were randomly distributed throughout the system area and assigned a discrete speed value i.e. 0/3/30/100 kms./hr with initial transmit power (maximum allowed power). The UEs get attached to the most appropriate BS depending on the handover margin, smallest PL, antenna gain, and log-normal fading. The connected UEs (active) were scheduled for every snapshot and allocated a certain amount of resources according to the QoS requirement. Every BS goes through with all MSs on its served mobile list and try adding their requested sub-carriers until all MSs are served or number of available sub-carriers exceed the maximum limit. In the latter case, the BS discards the last MS and tries connecting the next mobile in line which may have less required number of sub-carriers. This is equivalent to modelling a round robin (RR) scheduler with a full buffer traffic model. The use of RR scheduling with power control achieves more gain as compared to channel aware scheduling such as proportional fair (PF) [24].

In [32], the UL power control is defined as follows:

$$P_t = P_{max}\mathbf{1}, max[R_{min}, (\frac{PL}{PL_{x-ile}})^{\gamma}] \quad (5)$$

where P_t is the transmit power of the UE in dBm, P_{max} is the maximum allowed transmit power in dBm, R_{min} is

TABLE 1. Simulation parameters.

Parameters	Values
Network Topology	7 Cells, wrap around
Inter-Site Distance	433m
Carrier Frequency	2000 MHz
System Bandwidth	10 MHz
BS Antenna Gain	15 dBi
UE Antenna Gain	0 dBi
BS Antenna Height	30m
UE Antenna Height	1.5m
Propagation Model	Urban-Macro: 121.8+37.6*log10(d) dB (d is the distance from BS to UE in kms)
Traffic Model	full buffer
Scheduling algorithm	Round Robin
UE Speed	0/3/30/100 kms/hr
Log-normal Shadowing (shadow fading variance)	10 dB without correlation
Minimum Coupling Loss	70 dB
Handover Margin	3 dB
Number of Available RBs	24
RB Bandwidth	375 kHz
Number of RBs per UE	3
Number of UEs per cell	8
Handover Margin	3 dB
Thermal Noise Density	-174 dBm/Hz
UE noise Figure	9 dBm
Max BS transmit power	46 dBm
Max UE transmit power	24 dBm
Min UE transmit power	-30 dBm
Link Performance model	Attenuated and truncated form of the Shannon bound

the minimum power reduction ratio to prevent UEs having good channel condition to transmit at low power level i.e. $R_{min} = Pmin/P_{max}$. PL is the path-loss in dB between UE and serving BS. PL_{x-ile} is the x-percentile PL. With this PC scheme, the x percent of UEs that have a $PL > PL_{x-ile}$ will transmit at P_{max}. However, $0 < \gamma <= 1$ is the balancing factor for UEs with bad/good channel. The value of γ plays a vital role for the trade-off between cell-edge UE performance and overall spectral efficiency. If $\gamma = 0$, all UEs will be transmitting at P_{max}, resulting poor cell-edge performance. With $\gamma = 1$, the equation reduces to traditional slow power control resulting in poor spectral efficiency.

The SINR for each UE with respect to link-to-system-level mapping is given as follows [33]:

$$SINR = \frac{C(j,k)}{I(j,k)} = \frac{P_t(j,k) * pathloss_{effective}(UE_{j,k}, BS_j)}{I_{inter}(j,k) + I_{ext}(j,k) + N_t(thermal - noise)} \quad (6)$$

where $C(j,k)$ is the received power at j^{th} serving eNodeB from the intended k^{th} UE, $P_t(j,k)$ is the transmit power in dBm and $pathloss_{effective}$ is the effective path-loss which considered minimum coupling loss (MCL) as defined in [33].

The combined ICI and ACI at the victim reference cell is calculated as follows [33]:

$$I(j,k) = I_{inter}(j,k) + I_{ext}(j,k) + N_t(Noise_{thermal}) \quad (7)$$

where $I_{inter}(j,k)$ is the ICI coming from the UEs of adjacent cells operating on the same frequency sub-carriers and is calculated as follows:

$$I_{inter} = \sum_{l \equiv 1, l \neq j}^{N_{Cell}} p_t(l,k) * pathloss_{effective}(UE_{l,k}, BS_j) \quad (8)$$

$I_{ext}(j,k)$ is the ACI coming from the UEs on adjacent channels in coexistent LTE system. ACI is the combination of $I_{unwanted}$ (unwanted emission in adjacent band) and $I_{blocking}$ (blocking effect of receiver) and it is calculated as:

$$I_{ext} = \sum_{m \equiv 1}^{N_{ExtCell}} \sum_{v \equiv 1}^{k} iRSS_{blocking}(UE_{m,v}, BS_j) * iRSS_{unwanted}(UE_{m,v}, BS_j) \quad (9)$$

The effect of $I_{ext}(j,k)$ onto the system performance is set to be equal to zero, in order to make better relationship between SINR and ICI for CE learning.

The *achieved bit rate* for all uplink users is calculated as follows [33]:

$$BitRate = \frac{N_{sc_{per-UE}}}{N_{total-sc}} (x_{\frac{bps}{Hz}})_{SINR} \times BW_{MHz} \quad (10)$$

where $N_{sc_{per-UE}}$ and $N_{total-sc}$ are the number of allocated sub-carriers to each UE and total number of sub-carriers available at each base station (BS). The $x_{\frac{bps}{Hz}}$ is the spectral efficiency with respect to calculated *SINR* and BW_{MHz} is the bandwidth.

C. SCHEDULING

Once the C-eNodeB scheduler selects the UE and assigns RBs for uplink transmission, the embedded CE selects the optimal powers based on SINR and interference on scheduled RBs in subsequent TTI, such that the target SINR is achieved. In addition, the CE suggests the optimal transmit powers of UEs served by adjacent eNodeBs, operating on same scheduled RBs via X2-interface (a communication interface between eNodeBs). This process is depicted in Fig. 5 for 7 cell hexagonal layout. Note that the objective of embedded CE is to maximize the throughput of all attached UEs both interior/exterior under the constraints of given interference threshold. The throughput maximization under interference limitation is achieved by putting constraints on ICI environmental measurement parameter during optimization.

D. CE DESIGN

Fig. 6 illustrates the integration of RNN based learning and GA based reasoning. The optimization framework is summarized in Fig. 6(a), where the data is first collected for learning which helps GA based reasoning process to make optimal decisions. A simplified cognitive operation

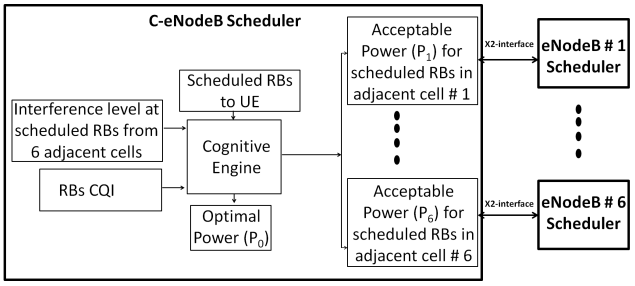

FIGURE 5. UE scheduling example.

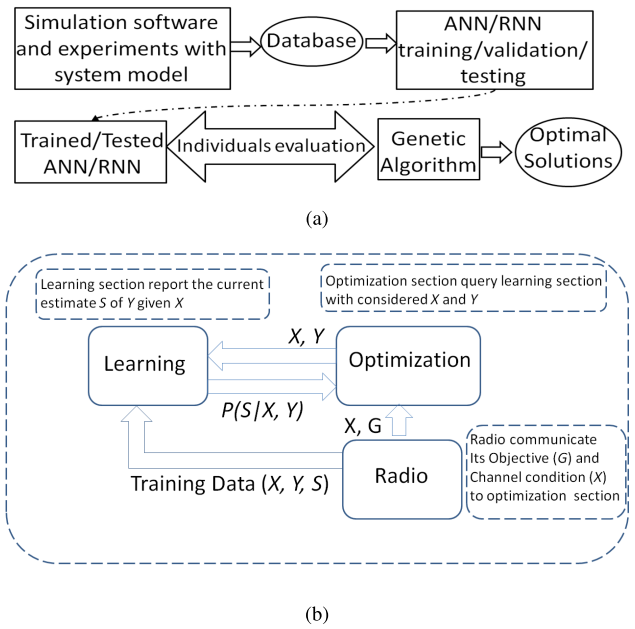

FIGURE 6. Cognitive engine operation. (a) Optimization framework: the data is first collected for learning which helps GA based reasoning process to make optimal decisions. (b) Integration of learning and optimization.

is illustrated in Fig. 6(b), where the decision is to be made based on given environment conditions and current radio objective. The learning module observes the channel X and estimates the performance S given radio configuration Y. The vectors X, Y, and S are the training parameters coming from the radio. The radio communicates with optimizer the required objectives and current channel quality information (CQI). The optimizer then queries the learning module with considered X and Y. The learning section returns the approximate performance of considered X and Y i.e. P(S|X, Y). Based on this report, the optimization section decides the optimal parameters. In this particular case, the RNN based learning agent is able to characterize the performances of different possible powers and channels combinations for serving users and adjacent cell users.

The information which is available to the cognitive controller can be classified into three categories: environmental measurements (external factors effecting the reliability of communication), configuration parameters (tuning knobs which can be changed in an optimal way to achieve desired performance), and the performance metric. Based on how different configuration parameters and environmental measurements are effecting the system performance, we fed the following configuration parameters and environmental measurements into the RNN black-box. The justification of selecting these parameters and environmental measurements is evident through (5-8), where a clear relationship among SINR, bit-rate, transmit power of intended UE, and transmit power of interfering UE can be seen.

- *Environmental measurements (X): SINR* and *ICI*
- *Configuration parameters (X):* Considered parameters are available channels (RBs) and transmit powers ($\boldsymbol{P_0}, \boldsymbol{P1}, \boldsymbol{P2}, \boldsymbol{P3}, \boldsymbol{P4}, \boldsymbol{P5}, \boldsymbol{P6}$) of all UEs served by C-eNodeB and adjacent 6-eNodeBs.
- *Performance metric (Y):* expected throughput for each C-eNodeB UE as a performance metric is considered.

With feature set X, label set Y, and n training samples $T = ((\boldsymbol{x_1}, \boldsymbol{y_1}), ., (\boldsymbol{x_n}, \boldsymbol{y_n})) \in (X\ x\ Y)^{\boldsymbol{n}}$, RNN creates a mapping $A: X \rightarrow Y$ from features to labels and predicts the labels for new samples. The estimate S given X, Y can be written as:

$$\boldsymbol{P(S|X, Y) = (P(X, Y|S)P(S))/(P(X, Y))} \qquad (11)$$

The UEs configuration parameters and environmental measurements as defined above are the inputs of RNN black-box and the performance metric is the output. The required input parameters are by default available at the cognitive eNodeB where the CE is embedded, with no extra computational effort required. Moreover, the scheduling process requires only one way communication/coordination which is from cognitive eNodeB to adjacent eNodeBs.

The designed CE can be used to address the ICI in LTE downlink system, and in fact, the downlink implementation of proposed approach would be much simpler.

V. PERFORMANCE EVALUATION

A. SIMULATION ASSUMPTIONS

The simulations have been performed using SEAMCAT-LTE simulator [33], Eclipse, and Matlab. SEAMCAT was used to accurately model the CR environment of our complex cognitive radio network and to build the dataset for training. Eclipse was used as a Java editor in order to extract the required parameters from the modelled scenario for post processing. We further developed the obtained source code for post processing and added some new classes and functions. Matlab was used for training and validation of neural networks. Learning rate for GD and LM was set to 0.01. The network was trained with the dataset of 7200 samples which has 3558 unique labels. A subset of dataset was used to train the neural network (NN) and rest of the data was used to compare the prediction performed by trained NN in face of new environmental condition (only for Test-Case I), which is elaborated further in CE testing subsection. The performance of learning process was evaluated using MSE, a difference between the predicted value and the actual value.

TABLE 2. ANN vs. RNN training performance.

Methods	Achieved MSE	Average time per iteration (s)	Total Training Time (s)	Number of iterations
ANN-GD	2.88 E-03	0.00581	33	10000
ANN-LM	1.37 E-06	0.0411	57	313
RNN-GD	6.9 E-04	4.62	566	121

TABLE 3. ANN vs. RNN testing performance: investigation of performance characterization ability in untrained scenarios.

Case	Scenario, Dataset, Unique Labels	Configurations	Mean Square Error ± Standard Deviation, 95% Confidence Interval		
			RNN-GD	ANN-GD	ANN-LM
I	Macro-OFDMA Urban propagation channel, dataset=7200, unique-labels=3558	Same as used for training	5.96E-04 ± 1.27E-03, (4.84-04, 7.08E-04)	2.04E-04 ± 4.55E-03, (2.86E-03, 3.66E-03)	1.31E-05 ± 3.20E-05, (1.12E-05, 1.65E-05)
II	Macro-OFDMA Urban propagation channel, dataset=8400, unique-labels=4160	change in active no. of UEs (from 8 users/cell to 12 users/cell)	8.19E-03 ± 7.87E-03, (8.02E-03, 8.35E-03)	1.719E-02 ± 2.02E-02, (1.07E-02, 1.76E-02)	1.52E-02 ± 1.40E-02, (1.49-02, 1.55E-02)
III	Macro-OFDMA Suburban propagation channel, dataset=1200, unique-labels=596	change in propagation channel from Urban to Suburban (Macro OFDMA)	2.22E-03 ± 2.59E-03, (2.10E-03, 2.40E-03)	8.32E-03 ± 1.22E-02, (7.63E-03, 9.01E-03)	5.82E-03 ± 6.27E-03, (5.46E-03, 6.17E-03)
IV	Macro-OFDMA Rural propagation channel, dataset=1200, unique-labels=642	change in propagation channel from Urban to Rural (Macro OFDMA)	7.60E-03 ± 2.95E-03, (7.54E-03, 7.66E-03)	1.10E-02 ± 6.66E-03, (1.08E-02, 1.91E-02)	1.20E-02 ± 3.65E-03, (1.19E-02, 1.21E-02)
V	Extended Hata Urban propagation channel, dataset=1200, unique-labels=517	change in propagation channel from Urban to Extended Hata	2.21E-02 ± 1.95E-02, (2.20E-02, 2.25E-02)	1.03E-01 ± 6.66E-02, (1.01E-01, 1.05E-05)	5.33E-02 ± 6.66E-02, (5.15E-02, 5.51E-02)
VI	Macro-OFDMA Urban propagation channel, dataset=1200, unique-labels=601	Same as system model but with fixed CEs training time (2s)	1.33E-02 ± 1.18E-02, (1.21E-02, 1.33E-02)	1.74E-01 ± 1.24E-01, (1.64E-01, 1.78E-01)	1.21E-01 ± 1.56E-02, (1.09E-01, 1.46E-01)

The main aim of CE training is to achieve least possible MSE in less training time which represents how well the CE has learnt the system behaviour.

B. CEs TRAINING

The CE was trained with ANN and RNN using the dataset obtained from the system model. The training with ANN is to demonstrate the coped challenges taking its performance as a reference for RNN. In training, different number of neurons, hidden layers and epochs were tried. The best performed RNN and ANN structures were 1 hidden layer with 6 neurons and 1 hidden layer with 20 neurons respectively. The training performance is illustrated in Table 2 where the least MSE achieved by ANN-GD is 2.88 E-03 in 10K iterations (33 s), ANN-LM achieved 1.37 E-06 in 313 iterations (57 s), and RNN-GD achieved the MSE of 6.9 E-04 in 121 iterations (566 s). The training performance of ANN-LM in terms of accuracy and training time was better than RNN-GD but ANN-LM/GD could only perform well for the trained cases, which is discussed in the following Subsection.

C. CEs TESTING

1) LONG-TERM LEARNING

The CEs were assumed to be working on a critical mission, where they do not have a privilege of retraining upon extreme propagation environment change. For such cases, long-term learning capability is essential which enables radio to adapt optimal radio parameters in a completely unknown scenario. To investigate the long-term learning, the CEs were tested in different wireless environments for which they were not trained. Table-3 illustrates six testing conditions along with the decision making accuracy of CEs. The testing conditions varied in urban, suburban, and rural propagation channels with different assumptions such as indoor, outdoor transmitter-receiver location, wall losses, losses between adjacent floors of the building, empirical parameters etc. Moreover, voice traffic variations with the assumption of training time constraints were also considered. Variation in electromagnetic environment effected the whole system in terms of average system throughput loss, average system SINR, internal/external interferences etc., which examined the decision making ability of the engines.

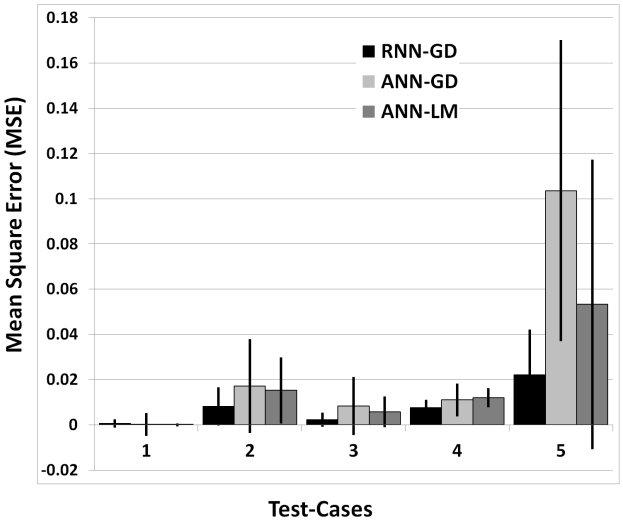

FIGURE 7. MSEs and SDs for Test-Cases I-V.

The critical analysis of RNN-GD, ANN-GD, and ANN-LM based CEs in both trained and untrained scenarios in terms of MSEs, squared errors (SEs), standard deviations (SDs), and confidence intervals (CIs) is illustrated in Table 3, Fig. 7, Fig.8, and Fig.9. All performance indicator metrics have shown the same trend i.e., in Test-Case I, ANN-LM outperformed RNN-GD mainly because of CE testing is conducted under a trained scenario. In all other test cases, as the electromagnetic environment changed, subsequently the performance of ANN started decreasing. Therefore, in Test-Cases (II-VI), RNN-GD with its long-term learning capability was up-to 87.53% accurate in making optimal and reliable decisions. In addition, small SE, MSE, SD, and CI of RNN based CE is apparent, particularly when electromagnetic environment differs more as compared to the trained scenario.

2) DECISION MAKING SPEED AT RUN-TIME

In real-time CE applications, fast decision making requires the CE to respond quickly upon severe wireless environment changes. As a core optimization algorithm, we not only require the decision accuracy but also the response speed. In training phase, the performance of ANN-LM was found to be faster but during run-time the RNN-GD outperformed ANN-LM/GD in total calculation time (decision making speed). This is mainly because of RNNs 3-level architecture in which the computation of output during run-time is extremely fast, since each neuron can be represented as a counter. Moreover, in RNN model, the neurons are represented as an integer rather than as a binary variable, which provides more detailed state representation [34]. In contrast, in ANN, the use of non-linear transfer function or activation function such as hyperbolic tangent and sigmoid takes more time to calculate as compared to RNN. Furthermore, the implementation of ANN is also difficult in hardware as compared to RNN.

The PSO+CBS approach presented in [8] showed the time consumption of 102.378s to complete 500 decisions at an average of 0.205s per decision. The integration of CBS reduced this time consumption to 54.632s at an average of 0.109s per decision. The RNN based CE consumed 1.4ms when it configured the radio parameters without interacting with GA based reasoning. In-contrast, ANN based CE and SEAMCAT simulator consumed 2.51ms and 4.61ms respectively. Therefore, RNN provided 44% and 66% faster decision making as compared to ANN and SEACMAT simulator. When ANN/RNN interacted with GA for optimized decision making, the time consumption raised to 0.5716s for RNN and 43.89s for ANN. It is to be noted that GA with ANN took much longer time to converge than with RNN, which is unreasonable. The GA+RNN time consumption was almost equal to PSO based decision making and slightly slower than PSO+CBS. However, PSO+CBS has limited learning, generalization, and robustness as discussed in Section-I. We believe that this time consumption can be further reduced up to 7.2ms from 0.316s, if we use cat swarm optimization instead of GA [35]. Table-4 summarizes the time consumption comparisons.

TABLE 4. Time consumption comparison for decision making.

Method	Average-time/decision (s)
PSO [8]	0.205
PSO+CBS [8]	0.109
RNN	0.0014
ANN	0.00251
ANN+GA	43.89
RNN+GA	0.5716

D. PERFORMANCE GAIN

1) FPC REFERENCE POINT SELECTION

Before the coverage-capacity gains comparison among ANN, RNN, and FPC, the best coverage-capacity trade-off case for FPC based method was determined. This was achieved by evaluating the FPC based power allocation over the range of different γ values. In the possible values of γ, there are two extreme cases, as stated in Section II, Subsection A. Fig. 10 shows the effect on transmit and receive power for these two cases, where high receiver dynamic range (P_{rx}) at BS for $\gamma = 0$ and vice-versa for $\gamma = 1$ is apparent.

Fig. 11(a and b) shows this effect by calculating the 5%-tile user throughput (coverage) and capacity. The least capacity of 14813 kbps and 2nd highest cell-edge throughput of 420 kbps for $\gamma = 1$ and the least cell-edge throughput of 83.9 kbps for $\gamma = 0$ is apparent. Yet, a trade-off can be achieved by setting γ between 0 and 1. The two best trade-off points are $\gamma = 0.6$ and $\gamma = 0.8$, where the highest achieved capacity is at $\gamma = 0.6$ with the cost of 16% less cell-edge throughput and the highest cell-edge throughput is at $\gamma = 0.8$ with the cost of 2% less capacity. In literature, researchers have shown different optimal choices for γ such as 0.5, 0.6, 0.7, and 0.8 [22], [36]–[38]. In our case, we found the best coverage-capacity trade-off at $\gamma = 0.8$ and taken it as a reference point for further investigation and comparisons.

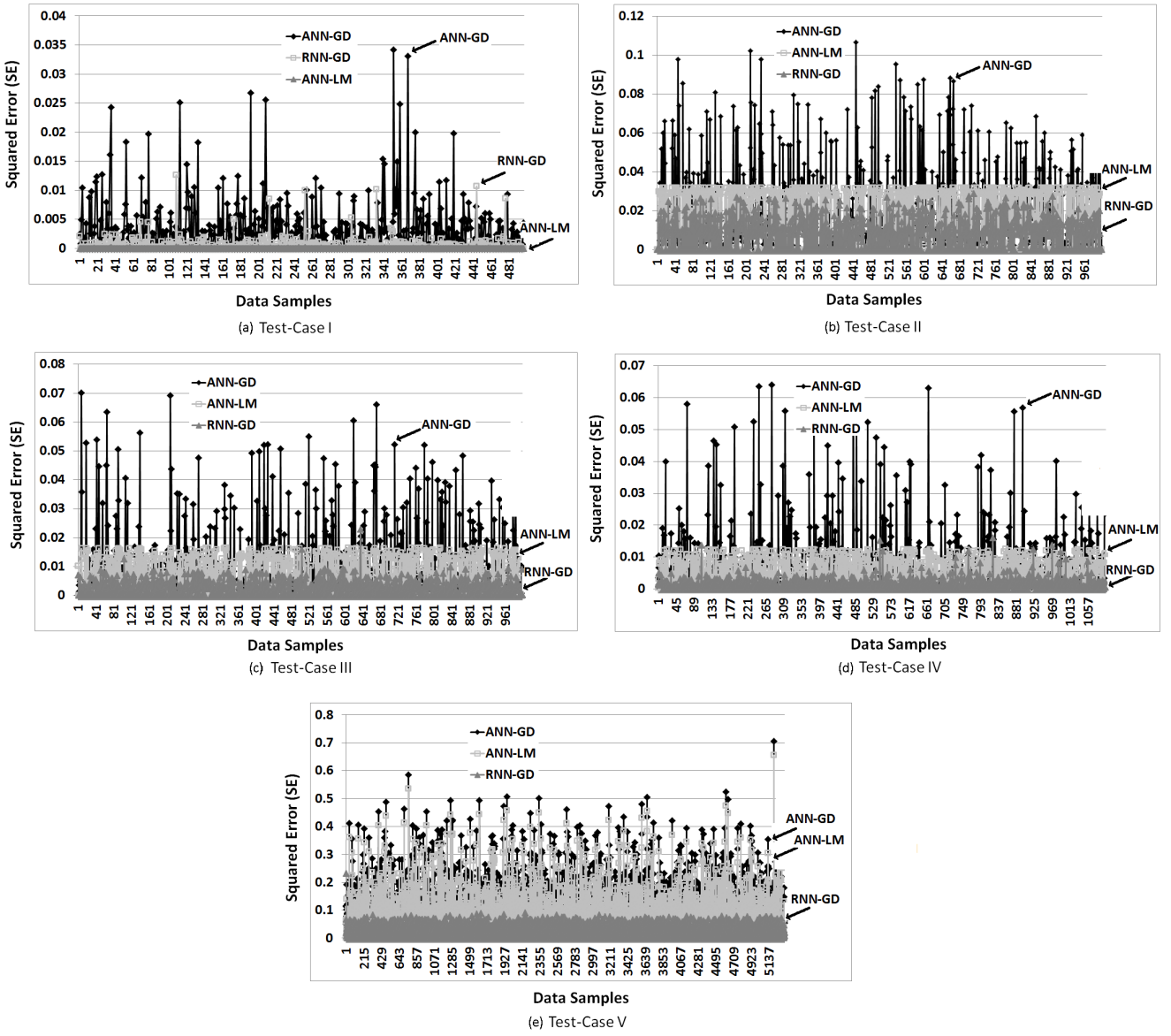

FIGURE 8. Squared Errors: (a)-(e) for Test-Cases I-V.

TABLE 5. 5%-tile, 25%-tile, and 50%-tile user throughput and average cell throughput [reference cell].

Methods	5%-tile	25%-tile	50%-tile	Average-cell (capacity)
FPC-0.4	270 kbps	1370 kbps	2140 kbps	14960 kbps
FPC-0.5	361 kbps	1412 kbps	2233 kbps	15152 kbps
FPC-0.6	385 kbps	1511 kbps	2150 kbps	15368 kbps
FPC-0.8	450 kbps	1548 kbps	2102 kbps	15028 kbps
FPC-1	420 kbps	1513 kbps	1920 kbps	14813 kbps
ANN	540 kbps	1517 kbps	2225 kbps	14560 kbps
RNN	360 kbps	1831 kbps	2500 kbps	17124 kbps

TABLE 6. 5%-tile, 25%-tile, 50%-tile user throughput and average cell throughput [entire system].

Methods	5%-tile	25%-tile	50%-tile	Average cell(capacity)
FPC	394 kbps	1710 kbps	2410 kbps	16182 kbps
ANN	134 kbps	1501 kbps	1997 kbps	14640 kbps
RNN	860 kbps	2072 kbps	2455 kbps	17294 kbps

2) FPC, ANN, AND RNN COVERAGE/CAPACITY COMPARISON

Figures 12 and 13 illustrate the cumulative distribution function (CDF) of average user throughput and capacity for reference cell. Table-5 illustrates the 5^{th}, 25^{th}, and 50^{th}%-tile user and average reference cell throughput. Fig. 14 illustrates the CDF of instantaneous user throughput in reference cell. Fig. 15 and Table-6 presents the 5^{th}, 25^{th}, and 50^{th}%-tile user and average cell throughput over entire system. It is to be noted that ANN provided more throughput to cell-edge users in reference cell by penalising the reference cell capacity up to 3% and overall exterior users throughput up to 65%. This is mainly because of high transmission power of cell-edge users in reference cell and corresponding high

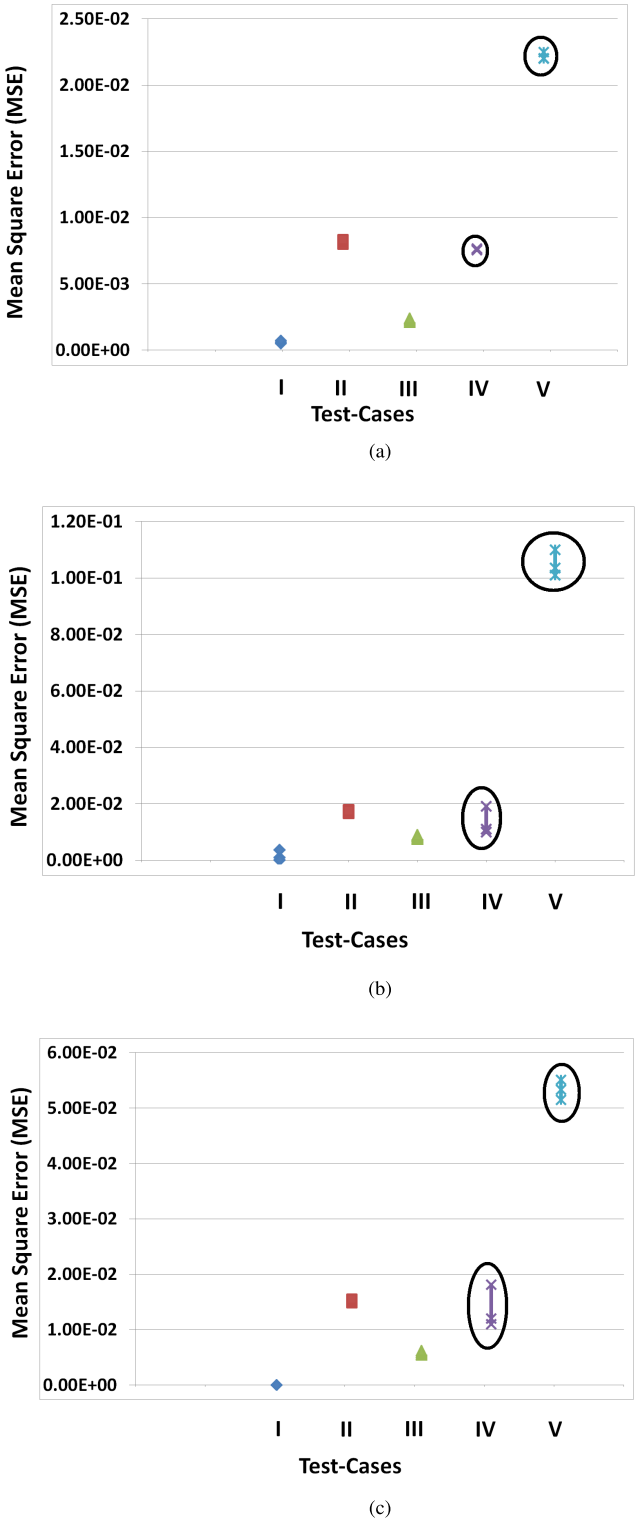

FIGURE 9. Confidence Intervals for Test-Cases I-V. (a) RNN-GD. (b) ANN-GD. (c) ANN-LM.

ICI to adjacent eNodeB users. In contrast, RNN based CE allocated less power to connected exterior and higher to interior users in reference cell. Therefore, benefited the reference cell capacity up-to 7% and overall exterior users performance up-to 118%. However, the RNN based CE penalises

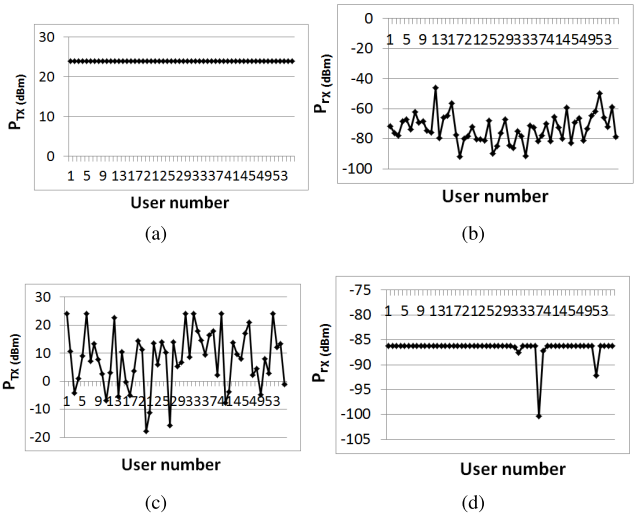

FIGURE 10. The transmit and receive power ranges for two extreme cases at $\gamma = 0$ (a and b) and $\gamma = 1$ (c and d).

TABLE 7. 5%-tile, 25%-tile, and 50%-tile user power consumption and average user power consumption in dBm.

Methods	5%-tile	25%-tile	50%-tile
FPC-0.4	10.103	15.733	18.647 3
FPC-0.6	3.160	11.462	16.259
FPC-0.8	-4.671	6.809	13.409
FPC-1	-12.184	2.221	10.341
ANN	-13.916	-1.098	8.6649
RNN	-22.527	-6.432	6.584

the cell-edge users of reference cell up-to 14%. Briefly, the RNN based CE achieved the maximum gain with minimum loss, whereas ANN achieved the minimum gain with maximum loss. Fig. 16 shows this trade-off more clearly, where the green colour refers to the high throughput of cell-edge users and red colour represents the low throughput of cell-edge users.

3) FPC, ANN, AND RNN USER POWER CONSUMPTION COMPARISON

Table-7 illustrates the 5^{th}, 25^{th}, and 50^{th}%-tile user power consumption for whole system. It can be seen that raising the power controlling factor reduces the user power consumption proportionally. Comparison of FPC with RNN has revealed approximately 8 dBm and 5 dBm less power consumption of cell-edge and centre users when they are attached with RNN based CE. Whereas, ANN based CE users have almost used the same power at cell-edges and slightly lower power on average as compared to FPC.

4) COMPARISON WITH EXISTING ICIC SCHEMES

The aforementioned analysis and comparison of RNN with ANN/FPC has revealed RNNs' significant gain in terms of both CCO and essential CE design features. For more in-depth analysis and comparison, we compared the performance of RNN with six different RRM/ICIC schemes namely Random, BSunc, RNC, RNC+BS, start index, and start index geometry weight, presented in [24].

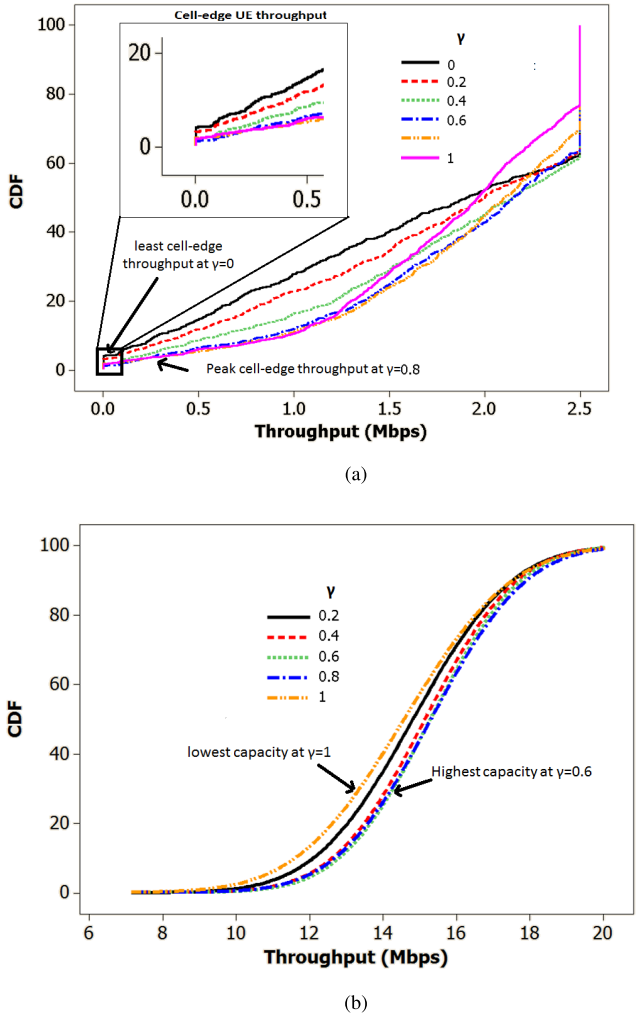

FIGURE 11. FPC based power allocation. Note: how the path-loss compensation factor γ controls the trade-off between fairness in cell-edge performance (cell-edge users throughput) and sectors to accumulate throughput. (a) User throughput. (b) Cell throughput.

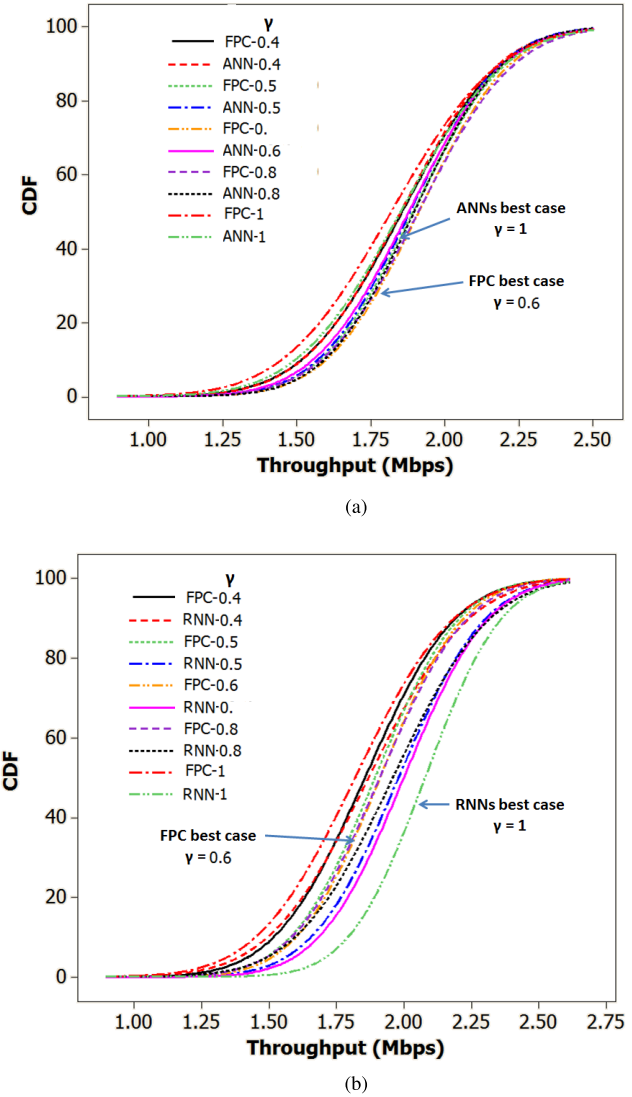

FIGURE 12. Average user throughput (reference cell). ANNs identical and RNNs better performance as compared to FPC is apparent. (a) FPC vs. ANN. (b) FPC vs. RNN.

In the Random allocation based RRM, BSs do not make use of instantaneous channel conditions with no ICIC. In RNC based RRM, a resource allocation algorithm operates within RNC and allocates optimal RBs and power allocation. BSunc uses opportunistic scheduling i.e., channel aware scheduling but without any RNC algorithm. The RNC+BS method schedules users who have favourable channel conditions and uses ICIC; therefore, it exploits both channel aware scheduling and the RNC ICIC algorithm. The ICIC start index and ICIC start index geometry weight algorithms provide slow time scale ICIC. The base line objective of these two algorithms is to avoid the cases where two users close to each other in adjacent cells use the same RB. This is avoided by coordinating the resource assignment with adjacent cells. In this approach, the operations and maintenance (O & M) centre divides the physical RBs into disjoint subsets. Afterwards, each cell is assigned to one of the subsets with starting index for interior/exterior users scheduling.

Table-8 illustrates the detailed comparison of first four RRM/ICCI schemes with RNN and FPC based methods in terms of used parameters for coordination, channel-aware scheduling, backhaul communication requirement, and capacity (50%-tile user throughput). It can be seen that the RNN based framework significantly outperformed Random, BSunc, and FPC methods with capacity improvements of 46%, 24%, and 15% respectively but with approximately the same cell capacity performance as compared to RNC and RNC+BS. However, RNC and RNC+BS methods have used both RBs and power as parameters for coordination. In addition, they require extensive coordination between eNodeBs and backhaul communication. Therefore, these methods restrict the widely accepted benefits of distributed resource allocation such as reduced deployment cost and mobile devices autonomy in making distributed

TABLE 8. FPC and RNN comparison with Random, BSunc, RNC, and RNC+BS based RRM/ICIC schemes.

Methods	ICIC	Parameters for coordination	Channel-aware scheduling	Backhaul communication	Capacity (50%-tile throughput) Mbps
Random	X	X	X	✓	10.105
BSunc	X	Power and RBs	✓	X	11.925
FPC	X	Power	✓	X	12.780
RNC	✓	Power and RBs	X	✓	14.810
RNC+BS	✓	Power and RBs	✓	✓	15
RNN	✓	Power	✓	X	14.824

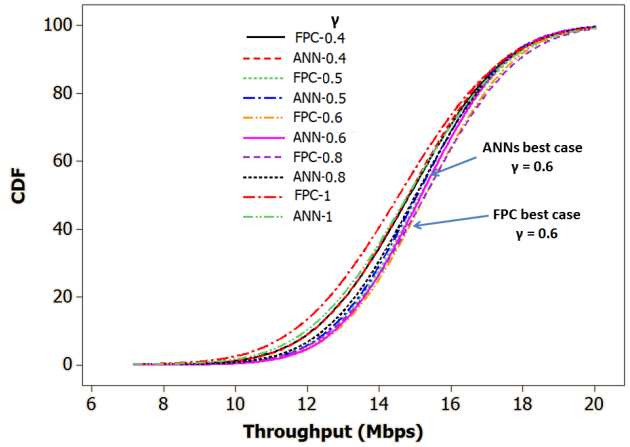

(a)

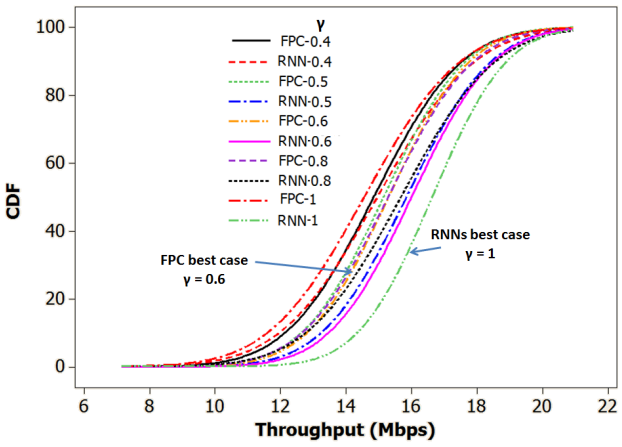

(b)

FIGURE 13. Instantaneous cell throughput (reference cell). ANNs identical and RNNs better performance as compared to FPC is apparent. (a) FPC vs. ANN. (b) FPC vs. RNN.

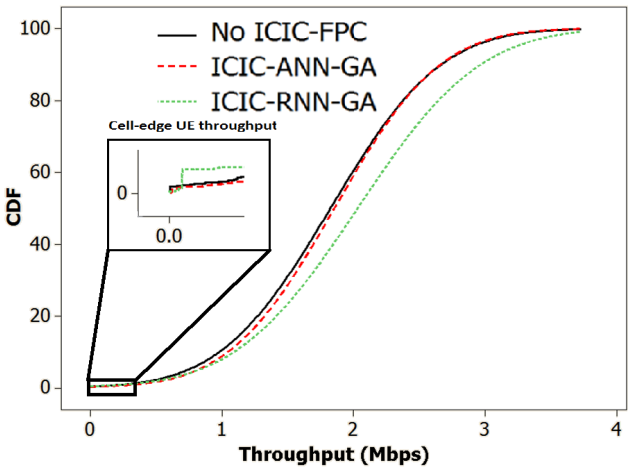

FIGURE 14. User throughput (reference cell).

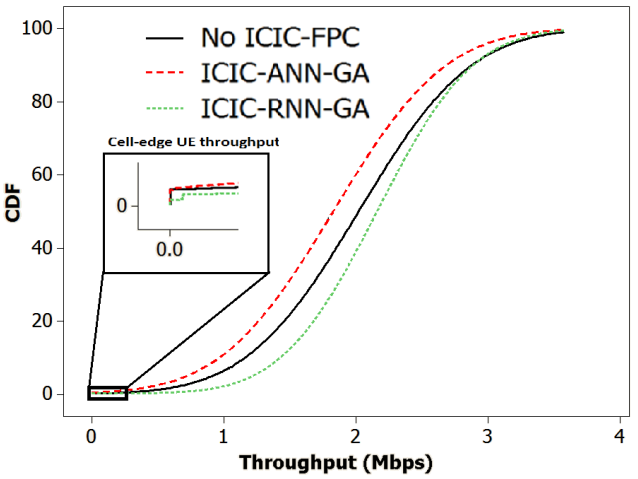

FIGURE 15. User throughput (system).

transmission decisions. In contrast, our proposed approach has used only power as a parameter for coordination and requires one way coordination/communication i.e., from reference cell to adjacent eNodeBs. Lastly, the authors in [24] have not mentioned the coverage performance of these approaches whether it was increased, decreased, or remained the same as compared to Random RRM algorithm. However, Fig. 17 illustrates the concurrent achievement of both coverage and capacity, where proposed framework achieved 20% more coverage as compared FPC based power allocation.

Table-9 illustrates the detailed comparison of ICIC start index and ICIC start index geometry weight algorithms with no-ICIC and RNN in terms of parameters for coordination, channel-aware scheduling, location-aware scheduling, frequency reuse value, backhaul communication requirements, and coverage gain. In [24], the authors reported 50-60% improvement in coverage as compared to no-ICIC method,

TABLE 9. FPC and RNN comparison with start index and start index geometric weight based RRM/ICIC schemes.

Methods	ICIC	Parameters for coordination	Channel-aware scheduling	Location-aware scheduling	Frequency reuse (exterior users)	Backhaul communication	Coverage gain
No-ICIC/start index or index geometric weight	✓	RBs	X	✓	3	✓	50-60%
No-ICIC/RNN	✓	Power	✓	X	1	X	118%

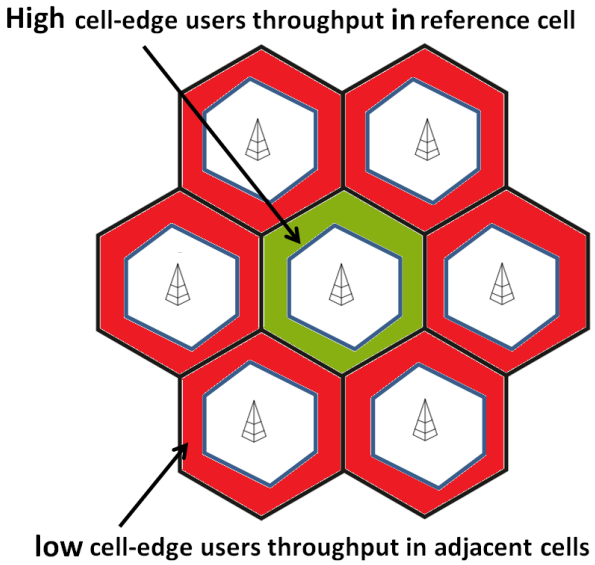

FIGURE 16. Cell-edge user throughput. (a) ANN. (b) RNN.

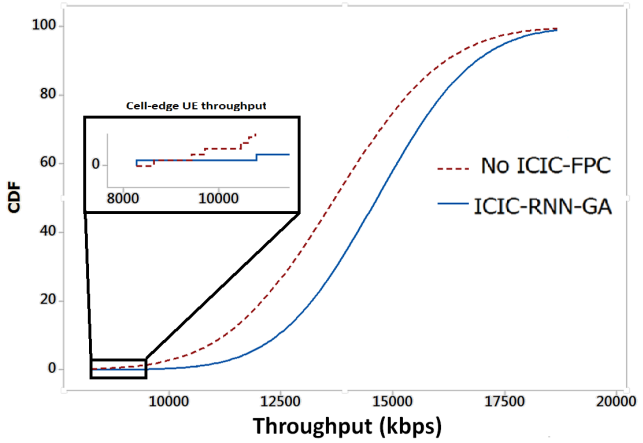

FIGURE 17. Cell throughput [24].

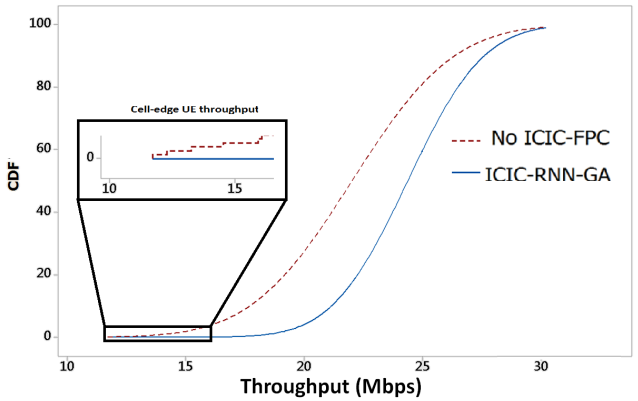

FIGURE 18. Cell throughput [28].

whereas RNN provided 118% better coverage as compared to no-ICIC. In contrast, our proposed framework reduced ICI with zero bandwidth loss (i.e. with frequency reuse of 1) as compared to the frequency reuse of 3 in start index and start index geometry weight algorithms. In addition, the less deployment cost due to no backhaul communication in the proposed framework is an obvious advantage over these two approaches.

The performance of proposed scheme has also been compared with [28]. The authors in [28] used fuzzy-RL to optimize the FPC parameters in SON manner and showed the capacity improvement of 10%. However, the authors reported no cell-edge performance and long-term learning capability. As stated in Section II.B that for realistic applications the generalization over the state-space is necessary which is insufficient in RL. In Fig. 7, 8, and 9 RNN has shown some extra ordinary generalization capabilities. In-addition, Fig. 18 illustrates the simultaneous capacity and coverage improvement of 10.78% and 28% respectively.

VI. CONCLUSION

In this paper, a power control technique based on RNN and GA is proposed to reduce ICI in cognitive radio systems. The critical analysis revealed that ANN based CE provided 20% more coverage to reference cell at the cost of 3% less reference cell capacity and 65% less overall system coverage. In contrast, RNN based CE provided 7% more average cell capacity and 118% more system coverage at the cost of 14% less coverage to reference cell. Moreover, RNNs 8 dBm and 5 dBm less power consumption by the cell-edge/centre users exhibited the usefulness of RNN based ICIC and RRM. The investigation of proposed CE architecture under CE design requirements showed that RNNs had 53% - 87% better long-term learning capability, reduction of 44% in response time for direct configuration settings, and quick convergence in 0.5716s as compared to 43s of GA+ANN. These results have showed that RNN based CE can be a reliable solution for real-time CR deployment. In future several other AI/ML techniques will be considered and more advanced models of RNN, both in terms of structure of the neural network and training algorithms. We believe the use of these methods applied to complex CR problems are one of the best tools available.

REFERENCES

[1] A. Katidiotis, K. Tsagkaris, and P. Demestichas, "Performance evaluation of artificial neural network-based learning schemes for cognitive radio systems," *Comput. Elect. Eng.*, vol. 36, no. 3, pp. 518–535, 2010.

[2] M. Bkassiny, Y. Li, and S. K. Jayaweera, "A survey on machine-learning techniques in cognitive radios," *IEEE Commun. Surveys Tuts.*, vol. 15, no. 3, pp. 1136–1159, Jul. 2013.

[3] A. S. Hamza, S. S. Khalifa, H. S. Hamza, and K. Elsayed, "A survey on inter-cell interference coordination techniques in OFDMA-based cellular networks," *IEEE Commun. Surveys Tuts.*, vol. 15, no. 4, pp. 1642–1670, Nov. 2013.

[4] R. Kwan and C. Leung, "A survey of scheduling and interference mitigation in LTE," *J. Elect. Comput. Eng.*, vol. 2010, Jan. 2010, Art. ID 1.

[5] A. Attar, V. Krishnamurthy, and O. N. Gharehshiran, "Interference management using cognitive base-stations for UMTS LTE," *IEEE Commun. Mag.*, vol. 49, no. 8, pp. 152–159, Aug. 2011.

[6] W. Jouini, C. Moy, and J. Palicot, "Decision making for cognitive radio equipment: Analysis of the first 10 years of exploration," *EURASIP J. Wireless Commun. Netw.*, vol. 2012, p. 26, Dec. 2012.

[7] H. I. Volos and R. M. Buehrer, "Cognitive radio engine training," *IEEE Trans. Wireless Commun.*, vol. 11, no. 11, pp. 3878–3889, Nov. 2012.

[8] X. Tan, H. Zhang, and J. Hu, "A hybrid architecture of cognitive decision engine based on particle swarm optimization algorithms and case database," *Ann. Telecommun.*, vol. 69, no. 11, pp. 593–605, 2014.

[9] A. Amanna, D. Ali, D. G. Fitch, and J. H. Reed, "Hybrid experiential-heuristic cognitive radio engine architecture and implementation," *J. Comput. Netw. Commun.*, vol. 2012, Jan. 2012, Art. ID 549106.

[10] M. Brehm and R. Prakash, "Proactive resource allocation optimization in LTE with inter-cell interference coordination," *Wireless Netw.*, vol. 20, no. 5, pp. 945–960, 2014.

[11] M. Simsek, M. Bennis, and I. Guvenc. (2014). "Learning based frequency- and time-domain inter-cell interference coordination in HetNets." [Online]. Available: http://arxiv.org/abs/1411.5548

[12] A. Galindo-Serrano and L. Giupponi, "Distributed Q-learning for aggregated interference control in cognitive radio networks," *IEEE Trans. Veh. Technol.*, vol. 59, no. 4, pp. 1823–1834, May 2010.

[13] S. Timotheou, "The random neural network: A survey," *Comput. J.*, vol. 53, no. 3, pp. 251–267, 2010.

[14] E. Gelenbe, Z. Xu, and E. Seref, "Cognitive packet networks," in *Proc. 11th IEEE Int. Conf. Tools Artif. Intell.*, Nov. 1999, pp. 47–54.

[15] E. Gelenbe, P. Liu, and J. Lainé, "Genetic algorithms for route discovery," *IEEE Trans. Syst., Man, Cybern. B, Cybern.*, vol. 36, no. 6, pp. 1247–1254, Dec. 2006.

[16] B. Oklander and E. Gelenbe, "Optimal behaviour of smart wireless users," in *Information Sciences and Systems*. New York, NY, USA: Springer-Verlag, 2013, pp. 87–95.

[17] E. Gelenbe and B. Oklander, "Cognitive users with useful vacations," in *Proc. IEEE Int. Conf. Commun. Workshops (ICC)*, Jun. 2013, pp. 370–374.

[18] A. Adeel, H. Larijani, and A. Ahmadinia, "Performance analysis of random neural networks in LTE-UL of a cognitive radio system," in *Proc. 1st Int. Workshop Cognit. Cellular Syst. (CCS)*, Koblenz, Germany, Sep. 2014, pp. 1–5.

[19] A. Adeel, H. Larijani, and A. Ahmadinia, "Efficient use of random neural networks for cognitive radio system in LTE-UL," in *Proc. 11th Int. Symp. Wireless Commun. Syst. (ISWCS)*, Barcelona, Spain, Aug. 2014, pp. 418–422.

[20] A. Adeel, H. Larijani, A. Javed, and A. Ahmadinia, "Critical analysis of learning algorithms in random neural network based cognitive engine for LTE systems," in *Proc. IEEE 81st Veh. Technol. Conf. (VTC Spring)*, May 2015, pp. 1–5.

[21] A. Adeel, H. Larijani, A. Javed, and A. Ahmadinia, "Random neural network based power controller for inter-cell interference coordination in LTE-UL," in *Proc. IEEE ICCW*, Jun. 2015, pp. 340–345.

[22] M. Boussif, N. Quintero, F. D. Calabrese, C. Rosa, and J. Wigard, "Interference based power control performance in LTE uplink," in *Proc. IEEE Int. Symp. Wireless Commun. Syst. (ISWCS)*, Oct. 2008, pp. 698–702.

[23] A. L. Stolyar and H. Viswanathan, "Self-organizing dynamic fractional frequency reuse for best-effort traffic through distributed inter-cell coordination," in *Proc. IEEE INFOCOM*, Apr. 2009, pp. 1287–1295.

[24] G. Fodor, C. Koutsimanis, A. Rácz, N. Reider, A. Simonsson, and W. Müller, "Intercell interference coordination in OFDMA networks and in the 3GPP long term evolution system," *J. Commun.*, vol. 4, no. 7, pp. 445–453, 2009.

[25] J. Shawe-Taylor and N. Cristianini, *Kernel Methods for Pattern Analysis*. Cambridge, U.K.: Cambridge Univ. Press, 2004.

[26] S. Deb and P. Monogioudis. (2013). "Learning based uplink interference management in 4G LTE cellular systems." [Online]. Available: http://arxiv.org/abs/1309.2543

[27] V. Poulkov, P. Koleva, O. Asenov, and G. Iliev, "Combined power and inter-cell interference control for LTE based on role game approach," *Telecommun. Syst.*, vol. 55, no. 4, pp. 481–489, 2014.

[28] M. Dirani and Z. Altman, "Self-organizing networks in next generation radio access networks: Application to fractional power control," *Comput. Netw.*, vol. 55, no. 2, pp. 431–438, 2011.

[29] E. Gelenbe, "Random neural networks with negative and positive signals and product form solution," *Neural Comput.*, vol. 1, no. 4, pp. 502–510, 1989.

[30] E. Gelenbe, "Stability of the random neural network model," *Neural Comput.*, vol. 2, no. 2, pp. 239–247, 1990.

[31] E. Gelenbe, "Learning in the recurrent random neural network," *Neural Comput.*, vol. 5, no. 1, pp. 154–164, 1993.

[32] 3GPP. (2009). *3rd Generation Partnership Project; Technical Specification Group Radio Access Network; Evolved Universal Terrestrial Radio Access (E-UTRA); Radio Frequency (RF) System Scenarios (Release 9)*. [Online]. Available: http://www.etsi.org/deliver/etsi_tr/136900_136999/136942/08.02.00_60/tr_136942v080200p.pdf

[33] (Jan. 2010). *ECOE Handbook, SEAMCAT*. [Online]. Available: http://www.cept.org/files/1050/documents/SEAMCAT%20Handbook%20January%202010.pdf

[34] E. Gelenbe and K. F. Hussain, "Learning in the multiple class random neural network," *IEEE Trans. Neural Netw.*, vol. 13, no. 6, pp. 1257–1267, Nov. 2002.

[35] P. M. Pradhan and G. Panda, "Comparative performance analysis of evolutionary algorithm based parameter optimization in cognitive radio engine: A survey," *Ad Hoc Netw.*, vol. 17, pp. 129–146, Jun. 2014.

[36] W. Xiao, R. Ratasuk, A. Ghosh, R. Love, Y. Sun, and R. Nory, "Uplink power control, interference coordination and resource allocation for 3GPP E-UTRA," in *Proc. IEEE 64th Veh. Technol. Conf. (VTC-Fall)*, Sep. 2006, pp. 1–5.
[37] R. Müllner, C. F. Ball, K. Ivanov, J. Lienhart, and P. Hric, "Contrasting open-loop and closed-loop power control performance in UTRAN LTE uplink by UE trace analysis," in *Proc. IEEE Int. Conf. Commun. (ICC)*, Jun. 2009, pp. 1–6.
[38] R. Müllner *et al.*, "Enhancing uplink performance in UTRAN LTE networks by load adaptive power control," *Eur. Trans. Telecommun.*, vol. 21, no. 5, pp. 458–468, 2010.

AHSAN ADEEL is currently pursuing the Ph.D. degree in wireless communication with the School of Engineering and Built Environment, Glasgow Caledonian University, U.K. His current research interests are in efficient radio resource exploitation mechanisms, intelligent network planning methods, cognitive radio, machine learning, MIMO–OFDM, and wavelet-based OFDM.

HADI LARIJANI received the Ph.D. degree in computer science from Heriot-Watt University, Edinburgh, U.K., in 2006. He is currently a Senior Lecturer with the Department of CCIS, School of Engineering and Built Environment, Glasgow Caledonian University. He has extensive experience in wireless communications and embedded hardware, including wireless communications, sensors, RF harvesting, and intelligent systems. He has been actively involved in scientific research for over 17 years participating in a number of projects in this area, including leading a major grant with IBM as an Industrial Partner developing Virtual Call Center agents. He holds several patents pending. His other areas of research interest are in performance evaluation of computer systems and networks, computer network simulation, software engineering, VoIP, LTE, cognitive radio, building energy management systems, and intelligent software agents. His work has resulted in over 50 international journal and conference publications.

ALI AHMADINIA received the Ph.D. degree from the University of Erlangen-Nuremberg, Erlangen, Germany, in 2006. From 2004 to 2005, he was a Research Associate with the Electronic Imaging Group, Fraunhofer Institute for Integrated Circuits, Erlangen. From 2006 to 2008, he was a Research Fellow with the School of Engineering and Electronics, University of Edinburgh, Edinburgh, U.K. In 2008, he joined Glasgow Caledonian University, Glasgow, U.K., where he is currently a Senior Lecturer in embedded systems. His research has resulted in more than 80 international journal and conference publications and nearly 1 million pounds worth of grants in the areas of reconfigurable computing, system-on-chip design, and wireless and DSP applications.